Relationship between ^{18}F-FDG uptake and heat shock protein 90α expression in colorectal cancer

Hyun-Yeol Nam[1] **MD, PhD,**
Hyoun Wook Lee[2] **MD, PhD**

1. Department of Nuclear Medicine
2. Department of Pathology, Samsung Changwon Hospital, Sungkyunkwan University School of Medicine, Changwon, South Korea

Keywords: ^{18}F-FDG -PET/CT
- Heat shock protein 90α
- Colorectal cancer

Corresponding author:
Hyoun Wook Lee MD, PhD
Department of Pathology, Samsung Changwon Hospital, Sungkyunkwan University School of Medicine, 158, Paryong-ro, Masanhoewon-gu, Changwon, 51353, South Korea
Tel: +82-55-233-6102
Fax: +82-55-233-5774
sudowo@naver.com

Received:
4 January 2021
Accepted revised:
10 March 2021

Abstract

Objective: We investigated whether heat shock protein 90α (HSP90α) expression is associated with fluorine-18-labeled fluoro-2-deoxy-D-glucose (^{18}F-FDG) uptake and whether ^{18}F-FDG positron emission tomography/computed tomography (PET/CT) can be used to predict the status of HSP90α expression in colorectal cancer (CRC). **Subjects and Methods:** The medical records and preoperative ^{18}F-FDG PET/CT studies of 51 patients with newly diagnosed CRC who underwent surgical treatment were retrospectively reviewed. The maximum standardized uptake value (SUVmax) of the primary tumor was calculated from the level of ^{18}F-FDG uptake. HSP90α expression was determined by immunohistochemistry. The relationship between SUVmax and HSP90α expression was analyzed. **Results:** Colorectal cancer with high HSP90α expression had significantly higher SUVmax than CRC with low HSP90α expression (18.88±10.06 vs. 12.38±5.04, P=0.003). There was a significant correlation between HSP90α expression and ^{18}F-FDG uptake (r=0.354, P=0.011). The highest accuracy for determining HSP90α status (68.6%) was obtained with a SUVmax cut-off of 15.4. Maximum SUV was the only predictor of HSP90α expression on multivariate logistic regression analysis (Odds Ratio=5.384, P=0.016). **Conclusion:** The expression status of HSP90α was significantly related to ^{18}F-FDG uptake in CRC.

Hell J Nucl Med 2021; 24(1): 10-17 *Epub ahead of print: 20 April 2021* *Published online: 30 April 2021*

Introduction

Heat shock protein 90α (HSP90α) is a molecular chaperone that ensures proper folding, maturation, and intracellular trafficking of numerous client proteins, such as ErbB2/Neu, Bcr-Abl, Raf-1, Akt, hypoxia-inducible factor (HIF)-1α, and mutated p53 [1]. Because many of these proteins are associated with the development and progression of cancer cells, many HSP90α inhibitors that block its chaperone activity exhibit potent anti-cancer activities by causing inactivation or/and degradation of client proteins [2].

Fluorine-18-labeled fluoro-2-deoxy-D-glucose (^{18}F-FDG) positron emission tomography/computed tomography (PET/CT) is a non-invasive molecular imaging modality widely used in cancer patients for initial staging, evaluating therapeutic response, detecting disease recurrence, and predicting survival outcomes [3]. The amount of ^{18}F-FDG uptake is the most reliable and widely used parameter to measure tumor metabolism and evaluate treatment response; fluorine-18-FDG uptake is reported semi-quantitatively as the maximum standardized uptake value (SUVmax) [4].

Colorectal cancer (CRC) is the third most common cancer and the second leading cause of cancer-related deaths worldwide [5]. Previous study showed that overexpression of HSP90 isoforms is involved in oncogenesis and is associated with tumor aggressiveness and poor prognoses in CRC [6]. Given their function, it seems likely, that both ^{18}F-FDG uptake and HSP90α expression are associated each other. However, to date, the relationship between ^{18}F-FDG uptake and HSP90α expression in CRC has not been reported, and the possible underlying mechanism is not clear. Accordingly, the present study investigates whether HSP90α expression is associated with ^{18}F-FDG uptake and whether ^{18}F-FDG PET/CT can be used to predict the status of HSP90α expression in CRC.

Subjects and Methods

Subjects

The institutional review board approved our study design and all informed consent exemptions. Patients were considered eligible if: (1) They were newly diagnosed with CRC from January 2015 to December 2016; (2) They had been treated by surgical resection at our institution; (3) The diagnosis of CRC had been confirmed by histopathologic examination of surgical specimens; (4) The HSP90α expression status of their tumor was determined by immunohistochemical staining of primary tumor tissue; (5) They had ^{18}F-FDG PET/CT study performed prior to surgery; (6) They had no adjuvant therapy administered before ^{18}F-FDG PET/CT study; (7) They had complete medical records. Fifty-one patients met these criteria. Their medical records, including data on age, sex, tumor size, TNM stage, tumor location, pathologic differentiation, and preoperative serum concentrations of carcinoembryonic antigen (CEA), were retrospectively reviewed and documented. Serum concentrations of CEA were not available in 8 patients.

^{18}F-FDG PET/CT protocol

All patients were examined using a dedicated PET/CT scanner (Discovery 710, GE Healthcare, Waukesha, WI, USA) within 7 days prior to surgical treatment. PET/CT imaging was performed 60min after injection of ^{18}F-FDG at a dose of 3.7MBq/kg (0.1mCi/kg) body weight. Before ^{18}F-FDG administration, patients were asked to fast for at least 6 hours. Blood glucose level at the time of ^{18}F-FDG injection was less than 160mg/dL in all patients. Sixty minutes after administration of ^{18}F-FDG, low-dose CT covering the area from the base of the skull to the proximal thigh was performed for attenuation correction and precise anatomic localization. Thereafter, an emission scan was conducted in three-dimensional mode. The emission scan time per bed position was 1.5min, and 7 or 8 bed positions were acquired. Positron emission tomography data were obtained using a high-resolution whole-body scanner with an axial view field of 15.7cm. The average axial resolution varied between 5.6mm (full width at half maximum) at 1cm and 6.3mm at 10cm. The average total PET/CT examination time was 15min. Computed tomography scans were obtained with a tube voltage of 120kVp and tube current of 30-180mAs. The PET data were iteratively reconstructed with attenuation correction and then reoriented in axial, sagittal, and coronal slices. For semi-quantitative analysis, irregular regions of interest were placed over the most intense area of ^{18}F-FDG uptake in primary tumors. Maximum SUV was calculated as (tissue activity per mL [Mbq/ml])/(injected dose [MBq]/body weight [kg]) on PET images.

Immunohistochemical analysis

Representative areas of tumors were marked on hematoxylin and eosin-stained slides and used for tissue microarrays (TMA). Two tissue cores per tumor with a diameter of 2mm were taken from donor paraffin blocks and put in blank recipient paraffin blocks. Tissue microarrays blocks were sectioned at 4μm for immunohistochemical staining using a Ventana Benchmark XT (Roche-Ventana, Tucson, AZ, USA). All sections were deparaffinized and subjected to pretreatment with CC1 (Roche-Ventana) for 60min at 100˚C. Sections were washed with reaction buffer followed by incubation with primary antibodies for 32 or 60min at 37˚C. Primary antibodies were against HSP90α (clone D7a, 1:100, Abcam, Cambridge, UK). An UltraView Universal DAB kit (Roche-Ventana) was used according to the manufacturer's recommendations to detect primary antibodies; this was followed by counterstaining with hematoxylin (Roche-Ventana). For the negative control, buffer was used instead of primary antibody. Expression of HSP90α was almost entirely cytoplasmic, and only cytoplasmic staining was evaluated to determine HSP90α expression. Cases were considered positive when 10% or more of tumor cells expressed the protein. The staining intensity of the positive cases was scored as 1 (weak), 2 (moderate), or 3 (strong). For statistical analyses, the negative and weakly positive cases were clustered in the low expression group, while the moderately and strongly positive cases constituted the high expression group.

Statistical analysis

Values are expressed as mean ± standard deviation or number. To compare between-group differences, the independent Student's t-test, Mann-Whitney U test, or Kruskal-Wallis test was used as appropriate when variables were continuous. Fisher's exact test or chi-square test was used for categorical variables. Multivariate logistic regression analysis was used to identify factors associated with HSP90α expression. Correlations between variables were tested using Spearman rho rank correlation analysis. Receiver-operating characteristics (ROC) curve analysis was used to assess the predictive value of SUVmax for HSP90α expression. All statistical analyses were performed using a statistical software package (MedCalc Ver. 14.12.0, MedCalc Software bvba, Ostend, Belgium), and statistical significance was established when the P value was 0.05 (two-tailed test).

Results

Patient characteristics

A total of 51 patients (28 males and 23 females; age 69.2±10.3 years, range 37-88) were enrolled. The mean primary tumor size was 5.0cm (range 0.7-10.0). Nineteen tumors were found in the cecum and ascending colon, 7 were found in the transverse colon, 1 was found in the descending colon, 16 were found in the sigmoid colon, and 8 were found in the rectum. Lymph node metastasis was detected in 28 patients. Distant metastatic lesions were detected in the liver (n=3), lung (n=1), small bowel (n=1), omentum (n=1), abdominal wall (n=1), left supraclavicular lymph node (n=1), and left axillary lymph node (n=1). According to the 8th edition of the American Joint Committee on Cancer TNM staging system [7], tumors were staged as follows: 7 as stage I, 16 as stage II, 19 as stage III, and 9 as stage IV. The staining intensity score of HSP90α expression was 0 in 22 patients, 1 in 12 patients, 2 in 6 patients, and 3 in 11 patients. Three patients with signet ring cell carcinoma had no HSP90α expression.

Relationships between clinicopathologic characteristics and ^{18}F-FDG uptake or HSP90α expression

The SUVmax for primary tumors ranged from 4.9 to 42.2 with an average of 14.55. Table 1 shows the relationship between clinicopathologic variables and SUVmax. Statistical analysis showed no significant differences in SUVmax according to age, sex, tumor size, serum CEA level, T category, lymph node or distant metastasis, location, or histologic type. Patients were categorized into 2 groups according to immunohistochemical staining of HSP90α: patients with high HSP90α expression (n=17) and patients with low HSP90α expression (n=34). No significant differences in age, sex, tumor size, serum CEA level, T category, lymph node or distant metastasis, location, or histologic type were found between the two groups (Table 2).

Table 1. *Relationship between clinicopathologic variables and SUVmax.*

Variables	No. of patients	Mean SUVmax	P
Age (years)			0.590
<70	18	13.76 ± 5.87	
≥70	33	14.98 ± 8.54	
Sex			0.115
Male	28	13.01 ± 5.70	
Female	23	16.42 ± 9.32	
Tumor size (cm)			0.133
<5	24	12.83 ± 7.39	
≥5	27	16.07 ± 7.71	
CEA (ng/mL)			0.896
<10	28	14.12 ± 8.52	
≥10	15	14.47 ± 7.54	
T category			0.144
T1/T2	8	10.90 ± 4.34	
T3/T4	43	15.23 ± 7.98	
Lymph node metastasis			0.537
Negative	23	13.81 ± 8.02	
Positive	28	15.16 ± 7.45	
Distant metastasis			0.491
Negative	9	16.17 ± 10.38	
Positive	42	14.20 ± 7.06	
Tumor location			0.235
Right	25	13.62 ± 7.87	
Left	26	15.45 ± 7.50	
Histologic type			0.644
Well differentiated	26	15.13 ± 7.98	
Moderately or poorly differentiated	22	14.38 ± 7.59	
Signet-ring cell	3	10.73 ± 6.30	

**SUVmax, maximum standardized uptake value; CEA, carcinoembryonic antigen; HSP90α, heat shock protein 90α.*

Relationship between ^{18}F-FDG uptake and HSP90α expression

Figure 1 shows representative cases of CRC with high and low HSP90α expression. Colorectal cancer with high HSP90α expression had a significantly higher SUVmax than CRC with low HSP90α expression (18.88±10.06 vs. 12.38±5.04, P=0.003, Figure 2). Colorectal cancers with high HSP90α expression were more frequent in the higher metabolic group (SUVmax> 15.4) than in the lower metabolic group (SUVmax≤15.4) (10/19 vs. 7/32, P=0.034). There was positive correlation between SUVmax and staining intensity of HSP90α (r=0.354, 95% CI=0.087-0.574, P=0.011). We next sought to determine the SUVmax threshold for optimal differentiation between these two groups. Receiver operating characteristic curve analysis revealed that the highest accuracy (68.6%) was obtained with SUVmax cut-off of 15.4, and the area under the curve was 0.708 (95% CI=0.564-0.827, P=0.012, Figure 3). Sensitivity and specificity for predicting HSP90α expression were 64.7% (95% CI=38.3-85.8) and 76.5% (95% CI=58.8-89.3), respectively.

Table 2. *Relationship between clinicopathologic variables and HSP90α expression.*

Variables	No. of patients	HSP90α expression		P
		High (n=17)	Low (n=34)	
Age (years)				0.757
<70	18	5	13	
≥70	33	12	21	
Sex				0.553
Male	28	8	20	
Female	23	9	14	
Tumor size (cm)				0.767
<5	24	7	17	
≥5	27	10	17	
CEA (ng/mL)				1.000
<10	28	10	18	
≥10	15	5	10	
T category				0.703
T1/T2	8	2	6	
T3/T4	43	15	28	
Lymph node metastasis				0.143
Negative	23	5	18	
Positive	28	12	16	
Distant metastasis				1.000
Negative	9	3	6	
Positive	42	14	28	
Tumor location				1.000
Right	25	8	17	
Left	26	9	17	
Histologic type				0.342

(continued)

Well differentiation	26	8	18	
Moderately or poorly differentiation	22	9	13	
Signet-ring cell carcinoma	3	0	3	
SUVmax				0.034*
≤15.4	32	7	25	
>15.4	19	10	9	
Mean ± SD		18.88 ± 10.06	12.38 ± 5.04	0.003*

**P<0.05. HSP90α, heat shock protein 90α; CEA, carcinoembryonic antigen; SUVmax, maximum standardized uptake value.*

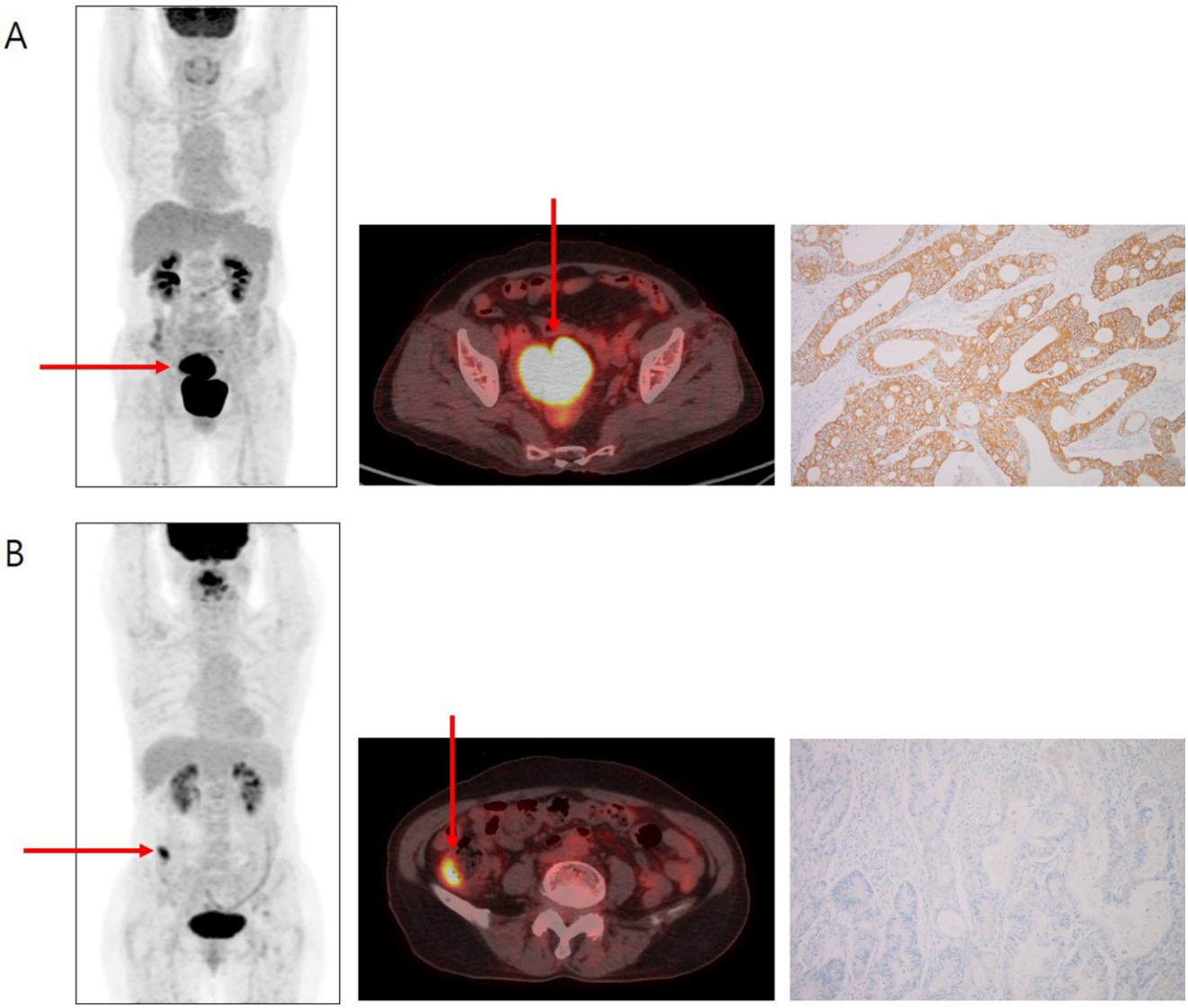

Figure 1. Images of maximum intensity projection (left), axial view (middle) of ^{18}F-FDG PET/CT and immunohistochemical staining (right) in representative cases. The SUVmax in colorectal cancer was higher (42.2 vs. 8.4) when HSP90α was highly expressed (A, intensity score; 3) than when HSP90α had low expression (B, intensity score; 0).

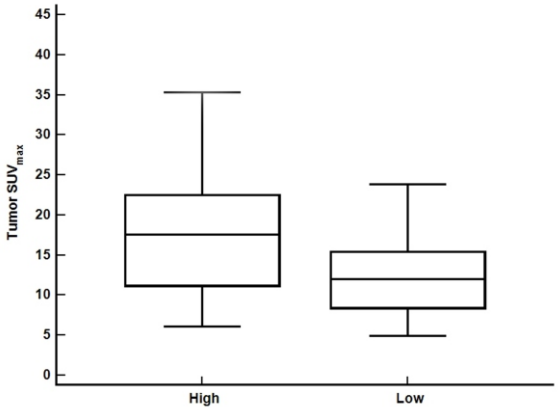

Figure 2. Box-and-whisker plots of tumor SUVmax according to HSP90α expression status in colorectal cancer (CRC). CRC with high HSP90α expression had significantly higher SUVmax than CRC with low HSP90α expression (18.88 ± 10.06 vs. 12.38 ± 5.04, P=0.003).

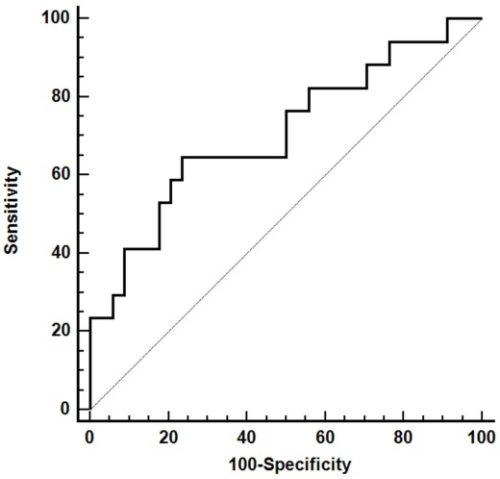

Figure 3. Receiver operating characteristic curve analysis of ability of SUVmax to predict HSP90α expression. Using cut-off value of 15.4, the sensitivity and specificity of SUVmax in predicting HSP90α expression were 64.7% and 76.5%, respectively. Area under the receiver operating characteristic curve is 0.708 (95% confidence interval=0.564–0.827, P=0.012).

Logistic regression analysis for independent predictive factors of high HSP90α expression

Multivariate logistic regression analysis was performed including factors with a P value of less than 0.15 on univariate analysis. The results revealed that SUVmax was the only significant predictor for high HSP90α expression (Odds Ratio= 5.384, P=0.016, Table 3).

Discussion

Heat shock proteins are a group of proteins that facilitate protein folding and maintenance of natural structures and functions of other proteins when cells are exposed to homeostatic challenges such as extreme temperature, anoxia, hypoxia, heavy metals, drugs, or other chemical agents that may induce stress or protein denaturation [8, 9]. Heat shock proteins are classified into several families according to their molecular mass [10]. Ninety kilodalton HSP (HSP90) is a representative family that is the most widely studied target for cancer therapy. Heat shock protein 90 includes different types of human isoforms such as cytoplasmic isoforms, HSP-90α (inducible) and HSP90β (constitutional), an endoplasmic reticulum isoform, glucose related protein 94, and a mitochondrial isoform, tumor necrosis factor (TNF) receptor-associated protein 1 (TRAP1) [10]. The inducible HSP90α isoform is a component of the invasive phenotype of cancer cells, indicating the importance of HSP90α for generating metastasis [6].

To the best of our knowledge, this is the first study to analyze the association between HSP90α expression and ^{18}F-FDG uptake in patients with CRC. Our results showed that the SUVmax in CRC was significantly higher when HSP90α was highly expressed than when HSP90α had low expres-

Table 3. *Logistic regression analysis for independent predictive factors of HSP90α expression.*

Variables	Univariate			Multivariate		
	OR	95% CI	P	OR	95% CI	P
SUVmax	3.968	1.160-13.579	0.028*	5.384	1.374-21.095	0.016*
Lymph node metastasis	2.700	0.780-9.347	0.117	3.919	0.961-15.982	0.057
Sex	0.622	0.193-2.009	0.428			
Age	1.486	0.425-5.195	0.535			
Tumor size	1.429	0.440-4.634	0.553			
T category	1.607	0.288-8.965	0.589			
Tumor location	1.266	0.394-4.063	0.692			
Histologic type	0.922	0.350-2.430	0.870			
CEA	0.900	0.240-3.379	0.876			
Distant metastasis	1.000	0.217-4.605	1.000			

**P<0.05. HSP90α, heat shock protein 90α; OR, Odds Ratio; CI, confidence interval; SUVmax, maximum standardized uptake value; CEA, carcinoembryonic antigen*

sion (18.88±10.06 vs. 12.38±5.04, P=0.003). SUVmax was positively associated with HSP90α expression (r=0.354, P= 0.011).

The association between HSP90α expression and ^{18}F-FDG uptake has not been reported until now. Because HSP90α is a molecular chaperone responsible for HIF-1α, the potential mechanism may be as follows. Hypoxia is common in many types of solid tumors, in which tumor cells rapidly proliferate and form large solid tumor masses, leading to obstruction and compression of surrounding blood vessels. HIF-1α is an oxygen-sensitive subunit, and its expression is induced under hypoxic stress conditions. Additionally, HIF-1α is more promoted by binding with HSP90α [11]. In rapidly growing tumor tissue, HIF-1α helps hypoxic tumor cells to shift glucose metabolism from the more efficient oxidative phosphorylation to the less efficient glycolytic pathway to maintain energy production [12]. For this reason, hypoxic cells tend to consume more glucose to meet their energy needs. HIF-1α mediates this metabolic conversion through induction of enzymes involved in the glycolysis pathway and overexpression of GLUTs, especially the GLUT1 isoform, which increases glucose import into tumor cells [13]. Therefore, more aggressive tumor cells have higher ^{18}F-FDG uptake through GLUT1. Previous studies suggested that GLUT1-mediated ^{18}F-FDG accumulation in CRC can predict the underlying tumor biology in terms of malignancy potential and overall prognosis [3, 14, 15]. Thus, it is likely that HSP-90α-positive CRC shows high ^{18}F-FDG uptake and is correlated with poor prognosis.

Heat shock protein 90α expression had no significant association with various clinicopathologic factors in our study. One possibility for our results is that HSP90α up-regulation might occur at early stages, similar to TRAP1, another isoform of the HSP90 protein family. It was previously suggested that up-regulation of TRAP1 is an early event in tumorigenesis that is already evident in high-grade adenomas and in situ carcinomas [16]. However, our results are in disagreement with previous studies. While Drecoll et al. (2014) reported that high HSP90 expression levels were associated with lower malignant potential [17], Chen et al. (2011) reported that HSP90 overexpression was correlated with metastasis [18]. Thus, further studies are needed to investigate these controversial findings.

Molecular targeting has become a prominent concept in cancer treatment and HSP90 has attracted attention as targets for novel anticancer strategies because of its crucial role in cancer biology [9, 10, 19]. Since geldanamycin, a 1,4-benzoquinone ansamycin antitumor antibiotic, was introduced as the first established inhibitor of HSP90, various HSP90 inhibitors have been tested in clinical trials. Heat shock protein

90 inhibitors have several advantages as anticancer drugs: (i) HSP90 inhibitors can simultaneously target multiple signaling pathways because many signaling proteins are HSP-90 client proteins, (ii) HSP90 inhibitors can target specific damage in tumor tissues with minimal toxicity in normal tissues, (iii) a combination of HSP90 inhibitors and proteasome inhibitors leads to accumulation of unfolded proteins that are insoluble and toxic to cancer cells [9]. Because HSP90α expression was positively associated with ^{18}F-FDG uptake in our study, the therapeutic effect of HSP90 inhibitor might be decided by evaluating SUVmax change before and after therapy. The utility of ^{18}F-FDG PET/CT for evaluating therapeutic response during HSP90 inhibitor therapy should be explored in future studies.

This study had some limitations due to its retrospective design. First, there were few enrolled patients, which weaken the strength of our findings. Second, we could not verify our assumption about the correlation between HSP90α expression and ^{18}F-FDG uptake because we did not investigate both HIF-1α and GLUT1 proteins. Third, we could not know whether CRC with high HSP90α expression demonstrates poor prognosis because follow-up data of enrolled patients was not collected. Despite these limitations, however, this is the first study to present evidence of the potential value of ^{18}F-FDG PET/CT scans for determining HSP90α expression status in patients with CRC, which contributes to clinical decision making on anti-HSP90 therapies.

In conclusion, we found a significant correlation between HSP90α and ^{18}F-FDG uptake in CRC. Receiver operating characteristic curve analysis indicated that ^{18}F-FDG uptake may have a role in predicting HSP90α expression. Multivariate logistic regression analysis revealed that SUVmax of the primary tumor was the only predictive factor of high HSP90α expression. These results suggest that ^{18}F-FDG PET/CT scans can be a useful complement for assessing the status of HSP90α expression in CRC.

The authors declare that they have no conflicts of interest.

Bibliography

1. Tsutsumi S, Neckers L. Extracellular heat shock protein 90: a role for a molecular chaperone in cell motility and cancer metastasis. *Cancer Sci* 2007; 98: 1536-9.
2. Goetz MP, Toft DO, Ames MM et al. The Hsp90 chaperone complex as a novel target for cancer therapy. *Ann Oncol* 2003; 14: 1169-76.
3. Jadvar H, Alavi A, Gambhir SS. ^{18}F-FDG uptake in lung, breast, and colon cancers: molecular biology correlates and disease characterization. *J Nucl Med* 2009; 50: 1820-7.
4. Park JS, Lee N, Beom SH et al. The prognostic value of volume-based parameters using ^{18}F-FDG PET/CT in gastric cancer according to HER2 status. *Gastric Cancer* 2018; 21: 213-24.
5. Kolligs FT. Diagnostics and Epidemiology of Colorectal Cancer. *Visc Med* 2016; 32: 158-64.
6. Milicevic Z, Bogojevic D, Mihailovic M et al. Molecular characterization of hsp90 isoforms in colorectal cancer cells and its association with tumour progression. *Int J Oncol* 2008; 32: 1169-78.
7. Amin MB, Edge SB, Greene FL et al. Eds. *AJCC cancer staging manual* 8th edn. Springer-Verlag, New York. 2017.
8. Macario AJ, Conway de Macario E. Molecular chaperones: multiple functions, pathologies, and potential applications. *Front Biosci* 2007; 12: 2588-600.
9. Wu J, Liu T, Rios Z et al. Heat Shock Proteins and Cancer. *Trends Pharmacol Sci* 2017; 38: 226-56.
10. Garcia-Carbonero R, Carnero A, Paz-Ares L. Inhibition of HSP90 molecular chaperones: moving into the clinic. *Lancet Oncol* 2013; 14: e358-69.
11. Hur E, Kim HH, Choi SM et al. Reduction of hypoxia-induced transcription through the repression of hypoxia-inducible factor-1alpha/aryl hydrocarbon receptor nuclear translocator DNA binding by the 90-kDa heat-shock protein inhibitor radicicol. *Mol Pharmacol* 2002; 62: 975-82.
12. Warburg O. On respiratory impairment in cancer cells. *Science* 1956; 124: 269-70.
13. Denko NC. Hypoxia, HIF1 and glucose metabolism in the solid tumour. *Nat Rev Cancer* 2008; 8: 705-13.
14. Furudoi A, Tanaka S, Haruma K et al. Clinical significance of human erythrocyte glucose transporter 1 expression at the deepest invasive site of advanced colorectal carcinoma. *Oncology* 2001; 60: 162-9.
15. Sakashita M, Aoyama N, Minami R et al. Glut1 expression in T1 and T2 stage colorectal carcinomas: its relationship to clinicopathological features. *Eur J Cancer* 2001; 37: 204-9.
16. Maddalena F, Simeon V, Vita G et al. TRAP1 protein signature predicts outcome in human metastatic colorectal carcinoma. *Oncotarget* 2017; 8: 21229-40.
17. Drecoll E, Nitsche U, Bauer K et al. Expression analysis of heat shock protein 90 (HSP90) and Her2 in colon carcinoma. *Int J Colorectal Dis* 2014; 29: 663-71.
18. Chen WS, Lee CC, Hsu YM et al. Identification of heat shock protein 90α as an IMH-2 epitope-associated protein and correlation of its mRNA overexpression with colorectal cancer metastasis and poor prognosis. *Int J Colorectal Dis* 2011; 26: 1009-17.
19. Monazzam A, Razifar P, Ide S et al. Evaluation of the Hsp90 inhibitor NVP-AUY922 in multicellular tumour spheroids with respect to effects on growth and PET tracer uptake. *Nucl Med Biol* 2009; 36: 335-42.